IEEE Access
Multidisciplinary | Rapid Review | Open Access Journal

Received August 6, 2020, accepted August 21, 2020, date of publication August 25, 2020, date of current version September 4, 2020.

Digital Object Identifier 10.1109/ACCESS.2020.3019244

Marine Predators Algorithm for Parameters Identification of Triple-Diode Photovoltaic Models

MAHMOUD A. SOLIMAN[1], HANY M. HASANIEN[2], (Senior Member, IEEE), AND ABDULAZIZ ALKUHAYLI[3], (Member, IEEE)

[1]Department of Electrical Engineering, Faculty of Engineering, Menoufiya University, Shebin El-Kom 32511, Egypt
[2]Department of Electrical Engineering, Faculty of Engineering and Technology, Future University in Egypt, Cairo 11835, Egypt
[3]Department of Electrical Engineering, College of Engineering, King Saud University, Riyadh 11421, Saudi Arabia

Corresponding author: Mahmoud A. Soliman (dr.msoliman08@gmail.com)

ABSTRACT The precise electrical modeling of photovoltaic (PV) module is crucial due to the large-scale permeation of PV power plants into electric power networks. Therefore, a triple-diode photovoltaic (TDPV) model is presented to address all PV losses. However, the TDPV is mathematically modelled by a nonlinear *I-V* behavior, including nine-parameters that cannot be directly determined from the PVs datasheet due to the lack data offered by the PV manufacturers. This article presents a new application of the marine predators algorithm (MPA) to properly extract the electrical parameters of the TDPV model of a PV panel. The validity of the MPA-based TDPV model is widely appraised by the numerical analyses, which are carried out under various temperatures and solar irradiations. The optimal nine-parameters achieved using the MPA are compared with that realized by different optimization approaches-based PV model. For a realistic study, the numerical results and the measured data are compared for the marketable Kyocera KC200GT and Solarex MSX-60 PV panels. The efficacy of the MPA-based TDPV model is properly executed by checking its current error with that obtained from various models. With the MPA technology, a highly accurate model of any marketable PV module can be attained, which represents a new contribution to the sector of PV power systems.

INDEX TERMS Marine predators algorithm, photovoltaic modeling, photovoltaic power systems, solar energy, triple-diode model.

I. INTRODUCTION

Globally, clean energy sources have gained great attention due to tremendous key reasons, including the depletion of conventional fuels, climate concerns, political issues, and inclination to live in a friendly environment [1]–[3]. Solar photovoltaic (PV) technology is regarded as one of the largest renewable energy sources around the globe. Recently, huge economical improvements of the PV power industry have been inserted, resulting in a very pure future of this prospective energy technology. Key evolutions depicted the recent progress of the PV power industry. Lately, significant developments in the PV industry are prospering dramatically, owing to the strict cost reduction in the PV components, which points out the huge efforts spent in enhancing the efficiency of PV system industry [2]. According to the recent statistics of the PV market, the global installed PV capacity reached 512 GW at the end of 2018, which denotes an increase of 27% compared with 2016's record. It is expected that the global installed PV capacity will attain 2.8 TW by 2030 [4]. This indicates the huge-level permeation of such PV power systems into the electricity supply networks. In this regarding, the huge-scale PV power systems interlinked to the electricity networks need a rigorous study and precise modeling of PVs to address and analyze the dynamic impact of such PVs on the electric power system performance under different temperatures and irradiations, the performance of shaded PVs, and transient network situations. The PV module is mathematically simulated by a nonlinear *I-V* relationship, including a large number of unknowns due to the inadequate data offered by the PV manufactures [5].

The associate editor coordinating the review of this manuscript and approving it for publication was Dongbo Zhao.

The PV cell is a junction of P-N semiconductor material, which have three different regions, *i.e.*, quasi-neutral, space-charge, and defect regions. These regions have diffusion and recombination losses of the charge carriers. The PV model should express all losses in the PV cells. The ideal PV model is executed by a cell-generated photocurrent (I_{PV}), which is relevant to the solar irradiation that falls on it. However, real I_{PV} diverges because of the visual and electric losses within the P-N junction of the PV cell, leading to a single-diode PV (SDPV) model [6]. This model can represent the diffusion and recombination losses in the quasi-neutral region of emitter and majority zones. The main features of the SDPV model are the simple structure and its fast dynamic behavior. For achieving an accurate modeling of the PV panels, a double-diode PV (DDPV) model is presented to appear the losses in the quasi-neutral and space-charge of the P-N junction. In the recent decade, a triple-diode PV (TDPV) model came into sight to address the previous losses and recombination in defect regions and grain boundary, which represent all losses in three regions of the P-N junction of the PV cell, leading to a precise modeling of such PVs [7]. In the TDPV model of PV modules, there are nine parameters, which are I_{PV}, series resistance (R_s), parallel resistance (R_p), ideality factor for each diode (a_1, a_2, a_3), and leakage current for each diode (I_{o1}, I_{o2}, I_{o3}) [1]. Notably, the ideality factor is set for each non-ideal diode to attain the best I-V characteristic curve and its value is between 1 and 2 based on the material type and the physical construction of the PV cell [6]. Besides, it depends on the exact bulk recombination mechanism due to the boron-oxygen defect or the interstitial iron. Therefore, the using of these factors leads to achieve a precise modeling of such PVs [8]. It is essential to properly extract the nine parameters to achieve influential and precise PV model that plays a decisive role in the dynamic behavior of grid-tied PV systems through simulation analyses.

Different approaches have been employed to fine-tune such unknown parameters of the PV model. In the recent literature survey, SDPV and DDPV models of PV modules are widely studied because of their lower unknowns which are determined using analytical techniques, iterative approaches, and meta-heuristic optimization approaches. Analytical techniques are applied to estimate the PV parameters using different selected-points, which are attainable from the PV datasheet, such as short-circuit current point (I_{SC}), open-circuit voltage point (V_{oc}), and maximum output power (P_m). Although these methods have a fast convergence speed and do not need any measurements, some derivations and approximations are integrated for reducing the number of unknowns, such as neglecting R_p [9], the initial values of R_p [10] and I_o [11], a Lambert function approach [12], and using the linear least-squares method [13]. However, these approaches suffer from the complexity and require various differentiation of dynamic equation, resulting in unrealistic solution. The analytical and meta-heuristic approaches are integrated to properly extract the DDPV model parameters of the PV modules [14], [15]. Moreover, several iterative algorithms are proposed to optimally fine-tune the unknown parameters of PV models such as Gauss-Seidel method [16] and Newton-Raphson with maximum likelihood estimator [17]. Notably, the previous mentioned approaches lack accuracy, leading to inexact values of these parameters due to the high non-linearity and multi-variable of such PV model [7], [8].

Recently, meta-heuristic approaches are developed to optimally attain the electrical parameters of different PV models of PV modules by minimizing the proposed cost functions. Genetic algorithm (GA) [18], hybrid trust-region-reflective algorithm [19], whale optimization algorithm (WOA) [7], improved WOA [20], improved chaotic WOA [21], hybrid firefly algorithm and pattern technology [22], and other heuristic algorithms [23]–[27] are widely applied to minimize the root mean square error and extract the PV model parameters. Moreover, a social network optimizer algorithm [28], a self-adaptive teaching-learning algorithm [29], and a multi-strategy success-history-based adaptive differential evolution [30] are presented to identify the parameters of different PV models. Various objective functions-based datasheet values have been proposed and utilized meta-heuristic approaches to overcome the previous mentioned problems, including bacterial foraging algorithm [31], differential evolution algorithms [32], [33], and shuffled frog leaping algorithm [34]. However, these techniques are not effective due to the range selection of upper and lower bounds of parameters, particularly the dark saturation current, which is sensitive because of its small values in micro-amperes.

At present, the TDPV model of the PV module has been utilized for precise modeling of the PV losses. The TDPV model includes nine-parameters, which are hardly to be recognized using analytical approaches due to the multi-variable and low number of nonlinear equations. Therefore, the optimization techniques play a vital role to identify these unknowns by minimizing the objective function. In the recent literature, various meta-heuristic optimizers are employed to properly extract the nine-parameters of the TDPV model like the sunflower optimization algorithm (SOA) [35], moth flame algorithm [36], WOA [7], harris hawks optimization algorithm [8], coyote optimization algorithm [37], and grasshopper optimizer algorithm (GOA) [38]. Besides, the integrated equation analysis and the SOA were presented to determine these parameters of the TDPV model [39]. According to the no free lunch theory, no optimizer can optimally reach the global optimum solution for all problems, which promotes the researchers to use various optimizers for extracting the unknowns of the TDPV model. This appears the main motivation of the authors to utilize the marine predators algorithm (MPA) to minimize the proposed objective function and hence extract the optimal nine-parameters of the TDPV model.

The MPA is a novel nature meta-heuristic algorithm, simulated in 2020 by *Faramarzi, et al* [39]. It is motivated by the prevalent foraging pattern in ocean predators and the optimal confrontation rate policy in the relation between the

predator and the prey in marine ecosystems [39]. In MPA, the predator is looking for the prey, and at the meantime, the prey itself is searching for its food [40]. The predator and prey are sighted as search representatives. The marine predators follow the survival of the fittest strategy to increase their encounter rates with prey in marine ecosystems. In the stochastic process of meta-heuristics algorithms, such as the MPA, the next position is based on the current position and the transition probability to the next position. Different strategies have been presented to describe the behavior of marine predators. However, the tradeoff between the Lévy strategy and Brownian helps in finding the best optimization strategy that describes the MPA optimization process [39]. The velocity ratio of prey to predator is the key factor in transferring the optimization process from a stage to another. The high-velocity ratio is the prominent feature in the first stage, while the unity and low-velocity ratios are noticeable marks for the second and third stages. The MPA is a powerful heuristic algorithm that involves several merits, such as the lower number of designed variables, simple procedure, low computation encumbrance, significant convergence speed, near-global solution, flexibility, independence to the problem, and the gradient-free nature [40]. Recently, the MPA approach was successfully applied in many fields with the purpose of design optimization. The MPA was developed to design a robust strategy for large-scale PV array reconfiguration to mitigate the partial shading effect on the Performance of PV System [40]. In addition, the MPA was applied in forecasting the confirmed cases of Covid-19 [41]. Moreover, a hybrid Covid-19 detection model based on an improved MPA approach for X-Ray image segmentation was presented in [42]. Therefore, the MPA can be nominated as a superior algorithm that can be applied to solve many problems in the electric power systems.

This article presents a novel application of the MPA approach to minimize the proposed objective function with the purpose of extracting the unknown nine-parameters of the TDPV model of a PV panel. The validity of the MPA-based TDPV model is widely appraised by the numerical analyses, which are implemented under various temperatures and solar irradiations. The optimal nine-parameters achieved using the MPA are compared to that realized by various optimization approaches-based PV model. For a realistic study, the numerical results and measured data are paralleled for two marketable Kyocera KC200GT and Solarex MSX-60 PV panels. The efficacy of the MPA-based TDPV model is properly executed by checking its current error with that obtained from various models. With the MPA technology, a precise model of any marketable PV module can be attained. This appears a new contribution to the sector of the PV power systems. According to our knowledge, the MPA-based solar cell parameters extraction has not till now been mentioned in the solar literatures.

The article is organized as follows: Section II describes the model of PV module. In Section III, the objective function formulation is proposed. The MPA technology is clearly presented in Section IV. Section V depicts the simulation analyses and discussion. Finally, Section VI draws the conclusion.

II. MODEL OF PV MODULE

The precise electrical TDPV model of PV modules is offered for the PV power system simulation studies. The TDPV model is represented by photo-current source, three parallel diodes, and shunt and series resistances, as depicted in Fig. 1 [1], [7]. The PV panel has a nonlinear I-V relationship that can be expressed as follows [7], [8]:

$$\begin{aligned} I = I_{PV} - I_{O1}\left\{exp\left[\frac{V+IR_s}{a_1V_t}\right]-1\right\} \\ - I_{O2}\left\{exp\left[\frac{V+IR_s}{a_2V_t}\right]-1\right\} \\ - I_{O3}\left\{exp\left[\frac{V+IR_s}{a_3V_t}\right]-1\right\} - \frac{V+IR_s}{R_p} \end{aligned} \quad (1)$$

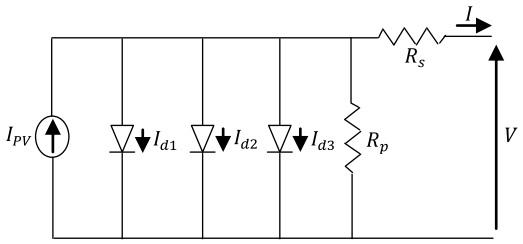

FIGURE 1. Equivalent circuit of TD model of PV module.

where I_{PV} is the cell-generated photocurrent, I_{Oi} stands for the leakage current of a diode i, a_i is an ideality factor for diode i, where i is the diodes number, *e.g.*, $i = 1, 2, 3$, V and I are the output voltage and the produced current of the PV module, respectively. R_s and R_p are the series and parallel resistances, respectively, and $V_t = N_sKT/q$. N_s equals the total number of cells in such panel, K is a Boltzmann coefficient ($1.3806503e^{-23}$J/K), T stands for the temperature of PV panel [K], and q denotes the electron charge ($1.60217646e^{-19}$C).

The remarkable points of the I-V characteristic, which are set in the PV datasheet, are I_{SC}, V_{OC} and P_m. Notably, several relations are proposed to depict the I-V relationship of different PV models of PV module under different environmental conditions as follows [43], [44]:

$$I_{PV} = \left(I_{PV,n} + K_i\Delta T\right)\frac{G}{G_n} \quad (2)$$

$$I_O = I_{On}\left(\frac{T}{T_n}\right)^3 e^{\left\{\frac{qE_g}{aK}\left[\frac{1}{T_n}-\frac{1}{T}\right]\right\}} \quad (3)$$

$$E_g = E_{g,n}\left(1 - 0.0002677\right)\Delta T \quad (4)$$

$$R_p = R_{P,n}\frac{G}{G_n} \quad (5)$$

where the variable subscript by n represent that these variables are determined at standard test conditions (STC). In the STC, $T = 25°$C and solar irradiation equals 1000 W/m^2.

K_i denotes the short circuit current-temperature factor, ΔT denotes the change between real and rated temperatures, G stands for the real solar irradiance, and E_g is the material band gap. $E_{g,n} = 1.211$ eV for the silicon cell [1], [2], [38]. Therefore, enormous efforts should be spent to extract the proper values of unknowns of the PV model. In this study, the unknown parameters of the TDPV model of PV panel are nine-parameters, which are I_{PV}, R_S, R_P, I_{Oi} and, a_i where $i = 1, 2, 3$.

III. OBJECTIVE FUNCTION FORMULATION

The electrical parameters of the TDPV model of PV module can be identified using the optimization approach, which essentially needs a definition of the objective function. The proper structure of the objective function is essential for precise identification of unknown parameters. The extracted parameters should guarantee that the model exactly simulates the PV panel. In this study, a novel objective function is proposed to optimally design the nine-parameters of such TDPV model. The current error, which represents the difference between the estimated and experimental model currents, is employed in this objective function. The objective function, ε, is the sum of three terms, which are the absolute current error, the squared current error, and the current error to the power of four. The ε is mathematically expressed as follows:

$$\varepsilon = \sum_{k=1}^{N} |f_k(V, I, \phi)| + \sum_{k=1}^{N} f_k^2(V, I, \phi) + \sum_{k=1}^{N} f_k^4(V, I, \phi) \quad (6)$$

where N denotes the sample number of the measured data, ϕ denotes the design variable vector including nine-parameters of such model that required to be computed. In the TDPV model, the $f_k(V, I, \phi)$ represents the current error, which is the difference between the measured current value and the estimated model current. The $f_k(V, I, \phi)$ can be mathematically expressed as follows:

$$\begin{aligned} f_k(V, I, \phi) = {} & I_{PV} - I_{O1}\left\{exp\left[\frac{V + IR_s}{a_1 V_t}\right] - 1\right\} \\ & - I_{O2}\left\{exp\left[\frac{V + IR_s}{a_2 V_t}\right] - 1\right\} \\ & - I_{O3}\left\{exp\left[\frac{V + IR_s}{a_3 V_t}\right] - 1\right\} \\ & - \frac{V + IR_s}{R_p} - I_{measured} \end{aligned} \quad (7)$$

where $\phi = \{I_{PV}, I_{O1}, I_{O2}, I_{O3}, R_s, R_p, a_1, a_2, a_3\}$

$I_{measured}$ denotes the current measured from the PV panel. The MPA technology is then employed to minimize the objective function, ε, to properly estimate these parameters. The principle MPA code is built with the help of using MATLAB environment [45].

IV. THE MPA TECHNOLOGY

MPA depends on the *survival of the fittest* strategy, in which predators have to select the optimum theory to exceed the confrontation rates related to the prey. In MPA, the predator is looking for the prey, and at the meantime, the prey itself is searching for its food [40]. Generally, the foraging strategy of many animals is a stochastic strategy, in which the next location relies on the current location and the probability transition to the next position. This optimal strategy has been developed by the marine ecosystem and has been selected by predators for surviving. The marine creatures, including sharks, swordfish, and tunas exhibit Lévy-like behavior in searching for prey, as the optimal search strategy for patchy prey in nature. The predators employ a Lévy approach in areas having lower gathering of prey and they use the movement of Brownian in an environment correlated to bountiful prey.

The MPA is a population-based approach. The initial randomization of the MPA is similar to different meta-heuristics algorithms, in which the candidate's position is updated as follows:

$$X_o = X_{min} + rand\,(X_{max} - X_{min}) \quad (8)$$

where X_{max} and X_{min} represent the upper and lower limit of design variable, respectively, and *rand* represents a random vector that its upper and lower bounds $\in [0, 1]$.

According to the *survival of the fittest* strategy, top predators have highly gifted in the foraging process. Therefore, the optimal solution is specified as a top predator to arrange *Elite*. Such *Elite* supervises of seeking and finding the prey related to the knowledge of prey's locations.

$$Elite = [X^I_{1,1} X^I_{1,2} X^I_{1,d}; \ldots\ldots; X^I_{n,1} X^I_{n,2} X^I_{n,d}] \quad (9)$$

where $\overrightarrow{X^I}$ is a vector of top predators that reproduced n times to arrange *Elite*. The variables n and d represent the agents number and dimensions, respectively. Such *Elite* is updated for each iteration if the top predator is replaced by another one that is better.

The *Prey* is arranged similar to the *Elite*'s dimension, in which the predators update their positions related to it. Simply, the initialization process establishes the initial *Prey*, where the fittest predator arranges the *Elite*. The *Prey* is depicted by the following:

$$Prey = [X_{1,1} X_{1,2} X_{1,d}; \ldots\ldots; X_{n,1} X_{n,2} X_{n,d}] \quad (10)$$

where $X_{i,j}$ is the j-th dimension of i-th prey. The optimization process mainly depends on the *Elite* and the *Prey*. Notably, the MPA applies random variables and operators for searching along with avoiding stuck into local minima.

A. MPA OPTIMIZATION PROCESS

In the MPA optimization process, three different phases are implemented in such process considering the entire life of the predator and prey in nature. The velocity ratio of prey to predator is the key factor in transferring the optimization process from a stage to another. The high-velocity ratio is the prominent feature in the first stage, while the unity and low-velocity ratios are noticeable marks for the second and third stages. A specific period of iteration is defined for each phase. These steps are assigned related to the rules

governed on the nature of predator and prey movement while mimicking the movement of predator and prey in nature. The three stages are discussed as follows [39]:

1) STAGE NO. 1: (HIGH-VELOCITY RATIO)

This stage happens when the prey is moving faster than the predator (a high-velocity ratio). Such scenario occurs in the initial iterations of the optimization process, in which the exploration issues are important. In the high-velocity (v≥10), the predator does not move, and the prey moves very fast searching for its food. The mathematical model of such phase is depicted as follows [39], [40]:

For $Iter < \frac{1}{3}Iter_{Max}$

$$\overrightarrow{stepsize}_i = \vec{R}_B \otimes \left(\overrightarrow{Elite}_i - \vec{R}_B \otimes \overrightarrow{Prey}_i\right) \tag{11}$$

where, $i = 1, 2, \ldots .n$

$$\overrightarrow{Prey}_i = \overrightarrow{Prey}_i + P.\vec{R} \otimes \overrightarrow{stepsize}_i \tag{12}$$

where v is the velocity ratio of prey to predator. $\vec{R}_B$ denotes a vector related to the normal distribution, illustrating the Brownian movement. Symbol $\otimes$ points out the entry-wise multiplications. P is a constant value of 0.5, and R denotes a vector that has random numbers of [0,1]. $Iter$ and $Iter_{Max}$ are the current and maximum iterations, respectively. This scenario occurs in the 1/3 iterations of the optimization process, where the step-size or movement speed is high for the high exploration ability [32].

2) STAGE NO. 2: (UNITY-VELOCITY RATIO)

In this stage, the predator and prey move at the same velocity. This scenario mimics that the predator and prey search for their food. That phase happens in the middle of the optimization process. In such scenario, the exploration and exploitation have half populations. In such scenario, the prey is in charge of exploitation and predator is responsible for exploration. For v $\approx$ 1, the prey moves in Lévy, while the predator moves in Brownian. This phase is mathematically described as follows [39]:

For $\frac{1}{3}Iter_{Max} < Iter < \frac{2}{3}Iter_{Max}$

For the first half of the population;

$$\overrightarrow{stepsize}_i = \vec{R}_L \otimes \left(\overrightarrow{Elite}_i - \vec{R}_L \otimes \overrightarrow{Prey}_i\right) \tag{13}$$

where, $i = 1, 2, \ldots .n/2$

$$\overrightarrow{Prey}_i = \overrightarrow{Prey}_i + P.\vec{R} \otimes \overrightarrow{stepsize}_i \tag{14}$$

where $\vec{R}_L$ denotes a vector of random numbers related to Lévy movement. The $\vec{R}_L \otimes \overrightarrow{Prey}_i$ mimics the prey motion with Lévy approach, where incorporating the step size of the prey location can mimic the prey motion.

For the second half of the population;

$$\overrightarrow{stepsize}_i = \vec{R}_B \otimes \left(\vec{R}_B \otimes \overrightarrow{Prey}_i - \overrightarrow{Prey}_i\right) \tag{15}$$

where, $i = n/2, \ldots .n$

$$\overrightarrow{Prey}_i = \overrightarrow{Elite}_i + P.CF \otimes \overrightarrow{stepsize}_i \tag{16}$$

where $CF = \left(1 - \frac{Iter}{Iter_{Max}}\right)^{\left(2\frac{Iter}{Iter_{Max}}\right)}$ is an adaptive variable for controlling the step size of the predator motion. The $\vec{R}_B \otimes \overrightarrow{Prey}_i$ mimics the predator motion by the Brownian approach, where the prey can update its location based on the predator motion in Brownian motion.

3) STAGE NO. 3: (LOW-VELOCITY RATIO)

On such phase, the predator moves faster than the prey. This is the last scenario in the optimization process that is related to the high exploitation process. In low-velocity ratio (v=0.1), the predator moves in Lévy. Such phase is mathematically described as follows [39]–[41]:

For $Iter > \frac{2}{3}Iter_{Max}$

$$\overrightarrow{stepsize}_i = \vec{R}_L \otimes \left(\vec{R}_L \otimes \overrightarrow{Elite}_i - \overrightarrow{Prey}_i\right) \tag{17}$$

where, $i = 1, \ldots .n$

$$\overrightarrow{Prey}_i = \overrightarrow{Elite}_i + P.CF \otimes \overrightarrow{stepsize}_i \tag{18}$$

The $\vec{R}_L \otimes \overrightarrow{Elite}_i$ mimics the predator motion by Lévy approach, while the step size is incorporated to *Elite* location to simulate the predator motion with the purpose of updating the prey's position.

B. EDDY FORMATION AND FADs' EFFECT

The eddy formation or Fish Aggregating Devices (FADs) effects are environmental matters that change the behavior of the marine predators. Based on the Filamlter' study [46], sharks take 80% of time in the near of FADs, and they take a long jump in various directions to probably find a region with another prey distribution in the rest 20% of their time. The FADs are local minima and have effect within the search space. The FADs effect is applied in the MPA to avoid trapping in the local optimum solutions, and can be mathematically expressed as follows [39], [41]:

$$\overrightarrow{Prey}_i = \begin{cases} \overrightarrow{Prey}_i + CF\left[\vec{X}_{min} + \vec{R} \otimes \left(\vec{X}_{max} - \vec{X}_{min}\right)\right] \otimes \vec{U} \\ \qquad\qquad if\ r \le FADs \\ \overrightarrow{Prey}_i + [FADs(1-r) + r]\left(\overrightarrow{Prey}_{r1} - \overrightarrow{Prey}_{r2}\right) \\ \qquad\qquad if\ r \ge FADs \end{cases} \tag{19}$$

where FADs is chosen 0.2. $\vec{U}$ is a vector that has arrays of zeros and ones. This vector is arranged by producing a random vector in [0,1] and varying this array to zero value if the array is <0.2 and to one if it is >0.2. $r \in [0,1]$. $\vec{X}_{max}$ and $\vec{X}_{min}$ are the vectors including upper and lower bounds of the dimensions. The subscripts ($r1$ and $r2$) stand for random indexes of *Prey* matrix.

C. MARINE MEMORY SAVING

The predator has a good memory to remember the location, where it has successfully been in foraging. After the *Prey* is updated and the effects of FADs are accomplished, this matrix is estimated to the fitness for updating *Elite*. For each

solution, the current fitness is compared to its previous value, and it can be replaced if it is better. In this case, the solution quality is improved [39]–[41]. Fig. 2 depicts the pseudo-code of MPA.

Initialize search agents (Prey) populations $i = 1,\ldots,n$
While *termination criteria are not met*
Calculate the fitness and construct the Elite matrix
If $Iter < Iter_{Max}$
Update prey based on Eq. 11
Else if $Iter_{Max}/3 < Iter < 2 * Iter_{Max}/3$
For the first half of the populations $(i = 1,\ldots,n/2)$
Update prey based on Eq. 13
For the other half of the populations $(i = n/2,\ldots,n)$
Update prey based on Eq. 15
Else if $Iter > 2 * Iter_{Max}/3$
Update prey based on Eq. 17
End (if)
Accomplish memory saving and Elite update
Applying FADs effect and update based on Eq. 19
Accomplish memory saving and Elite update
End ***while***

FIGURE 2. Pseudo-code of the MPA approach.

V. SIMULATION ANALYSES AND DISCUSSION

The proposed MPA technology is employed to extract the electrical parameters of any commercial PV module. In the current article, the MPA-TDPV model is applied to find the electrical parameters of two famous practical PV modules, which are Kyocera KC200GT [47] and Solarex MSX-60 [48]. The main goal of using these well-known modules is to check the validity of the offered TDPV model. The characteristics of such practical PV panels, which are the short-circuit current point (I_{SC}), the open-circuit voltage point (V_{oc}), the maximum output power of PV panel (P_m), the maximum output current of PV module (I_m), the maximum output voltage of PV panel (V_m), the number of series PV cells in PV module (N_s), the short-circuit current-temperature factor (Ki), and the open-circuit voltage-temperature factor (Kv), are recorded under the STC, as depicted in Table 1.

In this study, the MPA algorithm is employed to minimize the fitness function, ε, in (6), where the number of iterations is set 1000. In the MPA approach, the number of search agents is 25, and the number of design variables is 9. The settings of the optimal parameters of MPA are compromised between the algorithm precision and its intricacy. These settings are always selected by the trial and error method, which is the most commonly used approach in the industry for adjusting the meta-heuristic algorithm parameters. After multiple runs in the optimization process for the aforementioned well-known PV panels, the MPA was terminated where the lowest fitness function value was finally satisfied. The convergence curves of the best fitness value of the objective function using the MPA approach for the two PV panels are depicted in Fig. 3(a) and (b). It can be noted here that the MPA approach has a fast convergence speed. Besides, these graphs are smoothly converged and records lower fitness values of 1.245e-14 and 7.458e-13

TABLE 1. Datasheet of two commercial PV modules at the STC.

Company	Kyocera [47]	Solarex [48]
Model	KC200GT	MSX-60
Cell Type	Multicrystal	Polycrystalline
P_m [W]	200	60
V_m [V]	26.3	17.1
I_m [A]	7.61	3.5
V_{oc} [V]	32.9	21.1
I_{sc} [A]	8.21	3.8
N_s [cell]	54	36
K_i [A/°C]	0.00318	0.00065
K_v [V/°C]	–0.123	–0.08

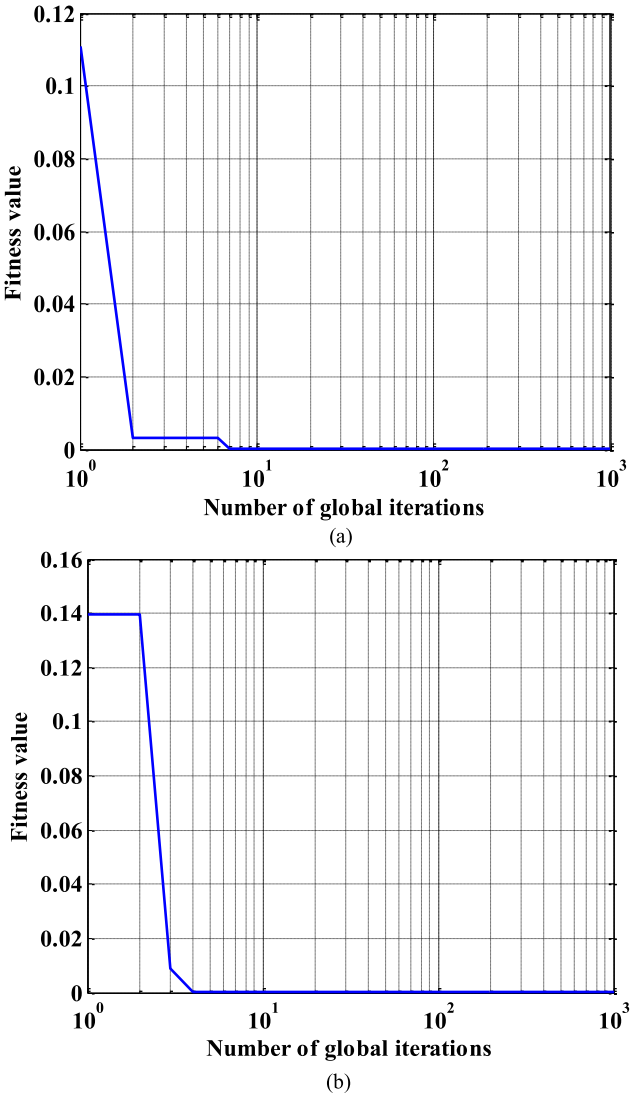

FIGURE 3. Fitness function convergence. (a) KC200GT. (b) MSX60.

for KC200GT and MSX-60, respectively. The optimization work and numerical results of this study are implemented using MATLAB 2016*b* [45]. Furthermore, a large number of independent runs around 50 of the proposed approach are performed to confirm the robustness of the proposed MPA technology. In this regard, the values of standard deviation, median, and variance through 50 individual runs are in close proximity to zero, which indicates the superiority and the adequate design of the MPA approach. The optimal design variables of the TDPV model for the KC200GT and MSX-60 PV panels are indicated in Table 2. Moreover, a fair comparison is done to confirm the validity of these optimal parameters of the offered TDPV model. In this regard, the optimal parameters of the MPA approach are compared with that achieved using the SOA, simulated annealing (SA), WOA, and GOA for the two well- known PV modules, as depicted in Tables 3 and 4. Note that, the optimal nine-parameters of TDPV model using the proposed MPA approach are nearly close to that obtained of other different algorithms for the two practical PV panels, and they are in an agreeable range of PV modelling preciseness. Besides, the optimal parameters are within acceptable range and there is no violation of the constraints of each variable. Futhermore, the fitness value of the proposed MPA-TDPV model is lower than that achieved using other approaches. So, the MPA-TDPV model is a competitive approach to the aforementioned established models. This reflects the superiority and the adequate design of the MPA.

TABLE 2. Optimal parameters using MPA-based proposed approach.

	KC200GT	MSX–60
I_{PV} [A]	8.19015	3.6741
R_p [Ω]	330.9143	280.1452
R_s [Ω]	0.3741	0.18745
a_1	1.3054	1.4012
a_2	1.214	1.0789
a_3	1.5412	1.4011
I_{O1} [A]	2.804e–08	2.81e–08
I_{O2} [A]	4.814e–10	3.52e–10
I_{O3} [A]	4.687e–10	4.16e–10

Furthermore, the proposed MPA-TDPV model is validated by comparing its numerical results with the measured data under different temperatures solar irradiations. The *I-V* and *P-V* behaviors of the offered MPA-TDPV model are compared with their measured data of the KC200GT PV module under various temperatures, as indicated in Fig. 4(a) and (b). These results are obtained under constant G = 1000 W/m^2. It is obviously recognized here that the numerical outcomes of the proposed MPA-TDPV model aligned with the experimental results. That indicates the efficient performance of the TDPV model of the PV panel. In addition, the *I-V* and *P-V* behaviors of the MPA-TDPV model as compared with their experimental results of the KC200GT PV module under various irradiations are illustrated in Fig. 5(a) and (b).

TABLE 3. Comparison of optimal TDPV model parameters for KC200GT.

	SOA [1]	SA [7]	WOA [7]	GOA [38]	MPA
I_{PV} [A]	8.21213	8.25	8.231	8.229174	8.19015
R_p [Ω]	606.1219	327.597	341.387	310.8623	330.9143
R_s [Ω]	0.23796	0.378	0.3421	0.2248107	0.3741
a_1	1.2481	1.199	1.32	1.219762	1.3054
a_2	1.991	1.2	1.236	1.091667	1.214
a_3	1.8421	1.48	1.0216	1.499932	1.5412
I_{O1} [A]	4.30e-8	1.78e–8	2.692e–8	2.888e-8	2.804e–08
I_{O2} [A]	2.22e-10	3.76e–10	4.678e–10	2.802e-10	4.814e–10
I_{O3} [A]	1.35e-6	4.62e–10	4.927e–10	2.797e-10	4.687e–10
Fitness value	1.23e-12	11.57e-8	9.8488e-8	9.977e-11	1.245e-14

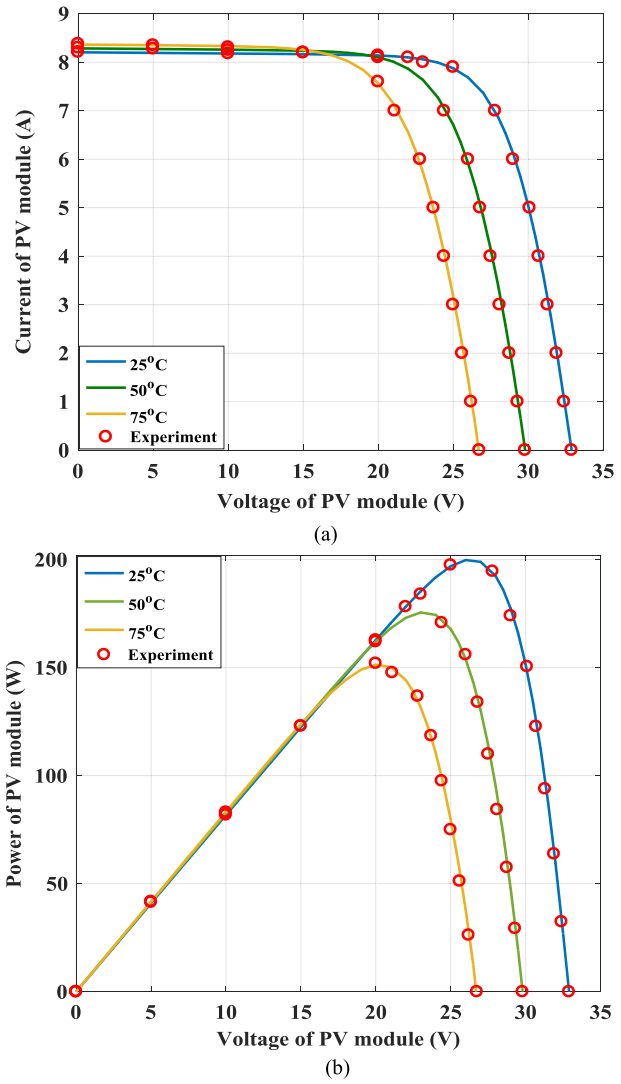

FIGURE 4. Numerical results and experimental data of the KC200GT PV module under different T, G = 1000W/m^2. (a) *I-V* curves. (b) *P-V* curves.

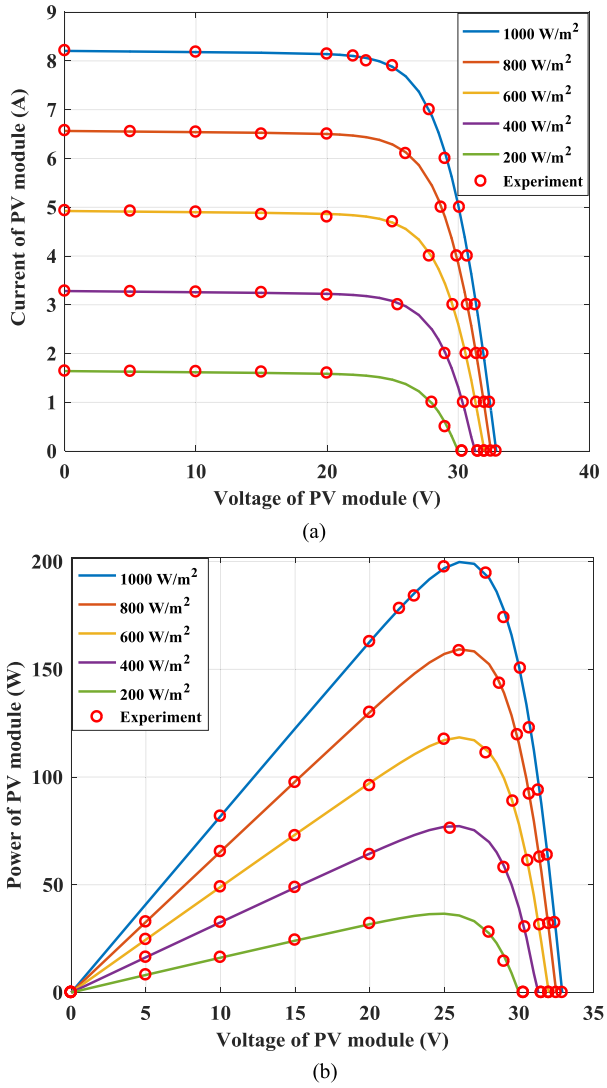

FIGURE 5. Numerical results and experimental data of the KC200GT PV module at different G, and T=25 °C. (a) *I-V* curves. (b) *P-V* curves.

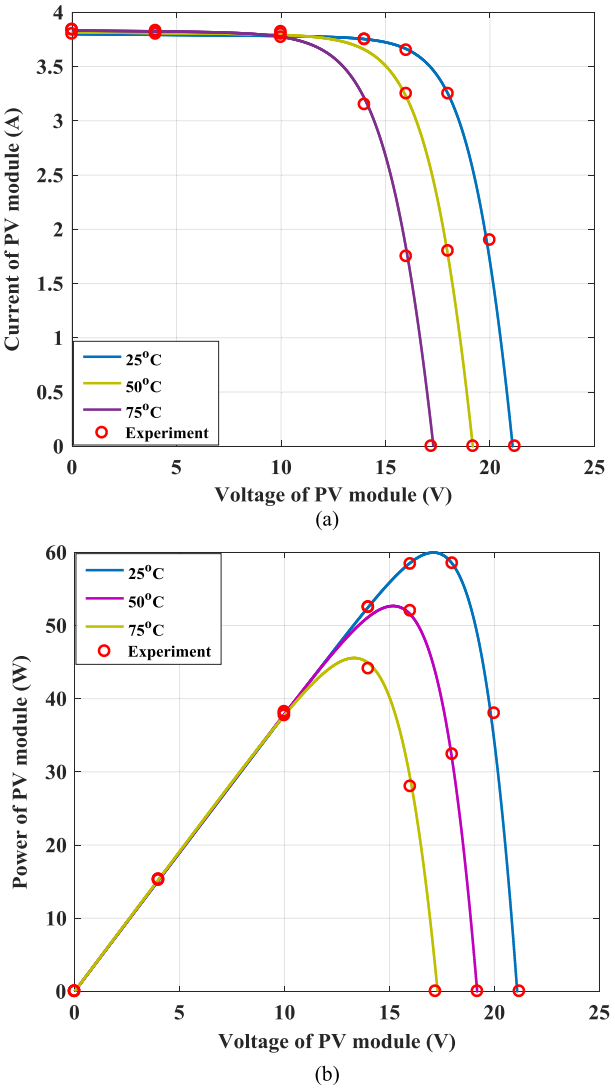

FIGURE 6. Numerical and experimental results of the MSX-60 PV module under different T, G = 1000W/m^2. (a) *I-V* curves. (b) *P-V* curves.

TABLE 4. Comparison of optimal TDPV model parameters for MSX-60.

	SOA [1]	SA [7]	WOA [7]	GOA [38]	MPA
I_{PV} [A]	3.80111	3.792	3.756	3.698	3.6741
R_p [Ω]	578.3468	298.59	277.37	349.8458	280.1452
R_s [Ω]	0.20598	0.211	0.195	0.1109557	0.18745
a_1	1.282	1.29	1.30	1.375876	1.4012
a_2	1.8043	1.22	1.23	1.074414	1.0789
a_3	1.4364	1.28	1.03	1.094849	1.4011
I_{O1} [A]	4.98e-8	1.98e–8	2.19e–8	2.18714e-7	2.81e–08
I_{O2} [A]	7.24e-10	4.76e–10	3.68e–10	2.294e-10	3.52e–10
I_{O3} [A]	1.42e-7	2.62e–10	3.97e–10	2.2108e-10	4.16e–10
Fitness value	1.12e-12	9.11e-10	7.316e-10	7.592e-10	7.458e-13

Notably, no deviations exist between the numerical and measured results. This reflects the efficacy of the novel MPA-TDPV model. The *I-V* and *P-V* relationships for a MSX-60 PV module that are achieved under constant G = 1000 W/m^2 and different temperatures using the proposed approach are compared with their experimental results, as illustrated in Fig. 6(a) and (b). Note that, the numerical results of the offered TDPV model using the MPA approach are very close to the experimental data. These comparisons can estimate the proposed TDPV model of PV panels and fairly access the effectiveness of the MPA.

It is worthy for noting here that all the measured data of the practical PV modules are realized on the outer surface of a Campus building roof. Fig. 7(a) depicts a practical KC200GT PV module used in the experimental test. The real PV panels are put into an open-glassed container, where a circulated cold or hot water is utilized in adjusting the ambient temperature of the PV modules, as clarified in Fig. 7(b). The experimental test was implemented during all day on 14 June 2017,

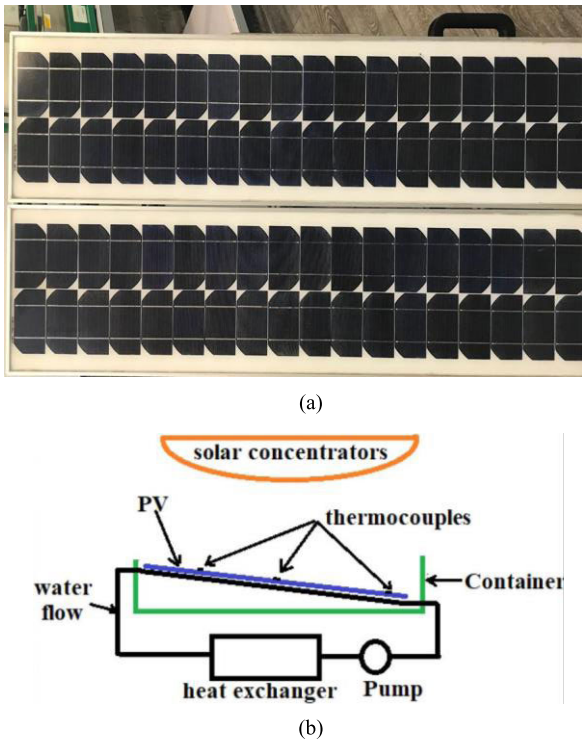

FIGURE 7. Experimental set-up. (a) Real KC200GT PV panel in the laboratory. (b) Temperature control of the PV.

in Faculty of Engineering, Ain Shams University, Cairo, Egypt. For both real PV modules, the I and V values are recorded under different environmental conditions using an ammeter and voltmeter measuring devices. Besides, the I and V values are measured at short-circuit, open-circuit, and various load conditions, where a variable resistor with a nominal value of 39 Ω is utilized. A silicon cell Pyranometer SP-110-SS is utilized to measure the solar irradiation. The SP-110-SS has a calibration element of 5 W/m^2 per mV and the calibration uncertainty is ±5%. In addition, the temperature is precisely recorded using a high probe infrared electronic thermometer temperature instrument with an accuracy of ±1°C, and its range is [−32, 550 °C].

For more verification of the offered model, the absolute current error (ACE) of the MPA-TDPV model relating to the measured data is paralleled with other approaches. The ACE of the proposed MPA approach as compared with the WOA [7] and the iteration method [49] for both the KC200GT and MSX-60 PV modules are pointed out in Fig. 8(a) and (b). It can be noticed here that the ACE of the MPA-TDPV model is very smaller than that of other approaches. So, the MPA-TDPV model is superior to these models, especially at the maximum power point and enclosure all practical applications of the PV modules. Thus, the high-efficiency and accuracy of the MPA-TDPV model reflect the suitable design of the MPA technology.

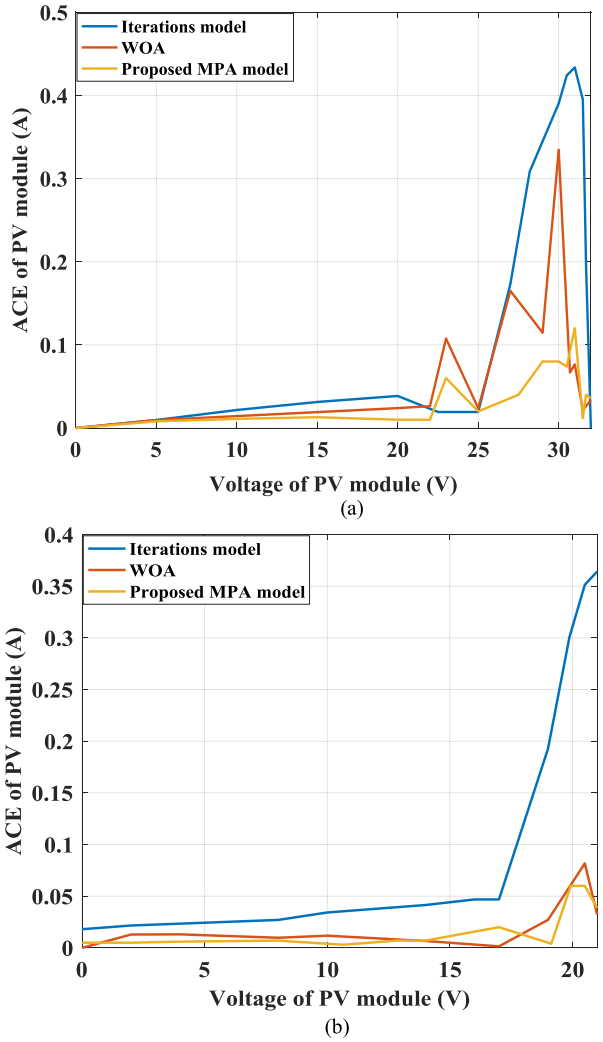

FIGURE 8. ACE of PV module. (a) KC200GT. (b) MSX-60.

VI. CONCLUSION

This paper has presented a novel objective function and a new application of the MPA approach to properly extract the nine-parameters of the TDPV model of the PV module. In this study, the main target is to obtain an accurate PV model for any commercial PV panel, which plays an essential role in the simulation studies of the grid-connected PV power systems. The mathematical modeling of the TDPV is expressed by a nonlinear I-V relationship, including nine-parameters that cannot directly determined from the PVs datasheet due to the shortage data offered by the PVs manufacturers. In this study, the problem formulation was expressed by the sum of three terms, which are the absolute current error, the squared current error, and the current error to the power of four. The main objective of the optimization problem is to minimize this function which represents the current error. The MPA technology was successfully utilized to minimize the objective function, obtaining the nine-parameters of the TDPV model of the PV module. Various comparisons were exhibited to check the efficacy of the offered TDPV model using the

MPA technology. The proposed algorithm was successfully employed to optimally design the parameters of two marketable KC200GT and MSX-60 PV modules. The optimal parameters, realized using the MPA-TDPV model, are coherent with that achieved using other different algorithms, where the MPA approach has recorded lower optimal fitness values of 1.245e-14 and 7.458e-13 for KC200GT and MSX-60 PV modules, respectively. Furthermore, the simulation outcomes of the MPA-TDPV model concur with the measured data for these well-known PV panels under several environmental situations. The ACE of the MPA-TDPV model indicates a lower value than other PV models for the marketable PV panels. This points out the superiority, efficacy, and robustness of the proposed approach for achieving a precise TDPV model-based PV panel. With the help of the MPA approach, an accurate modeling of any marketable PV panel can be realized. Moreover, the MPA technology can be further extended to solve different optimization problems in the power system applications, energy storage devices, and smart grids.

REFERENCES

[1] M. H. Qais, H. M. Hasanien, and S. Alghuwainem, "Identification of electrical parameters for three-diode photovoltaic model using analytical and sunflower optimization algorithm," *Appl. Energy*, vol. 250, pp. 109–117, Sep. 2019.

[2] M. H. Hasanien, "Performance improvement of photovoltaic power systems using an optimal control strategy based on whale optimization algorithm," *Electr. Power Syst. Res.*, vol. 157, pp. 168–176, 2018.

[3] R. N. Kalaam, S. M. Muyeen, A. Al-Durra, H. M. Hasanien, and K. Al-Wahedi, "Optimisation of controller parameters for grid-tied photovoltaic system at faulty network using artificial neural network-based cuckoo search algorithm," *IET Renew. Power Gener.*, vol. 11, no. 12, pp. 1517–1526, Oct. 2017.

[4] *PV Power Plants 2018 Global Industry Guide*. Accessed: Dec. 31, 2019. [Online]. Available: http://www.pvresources.com

[5] H. M. Qais, M. H. Hasanien, and S. Alghuwainem, "Transient search optimization for electrical parameters estimation of photovoltaic module based on datasheet values," *Energy Convers. Manage.*, vol. 214, Jun. 2020, Art. no. 112904.

[6] A. Coester, M. W. Hofkes, and E. Papyrakis, "Economics of renewable energy expansion and security of supply: A dynamic simulation of the German electricity market," *Appl. Energy*, vol. 231, pp. 1268–1284, Dec. 2018.

[7] O. S. Elazab, H. M. Hasanien, M. A. Elgendy, and A. M. Abdeen, "Parameters estimation of single-and multiple-diode photovoltaic model using whale optimisation algorithm," *IET Renew. Power Gener.*, vol. 12, no. 15, pp. 1755–1761, Nov. 2018.

[8] M. H. Qais, H. M. Hasanien, and S. Alghuwainem, "Parameters extraction of three-diode photovoltaic model using computation and Harris Hawks optimization," *Energy*, vol. 195, Mar. 2020, Art. no. 117040, doi: 10.1016/j.energy.2020.117040.

[9] V. Khanna, B. K. Das, D. Bisht, Vandana, and P. K. Singh, "A three diode model for industrial solar cells and estimation of solar cell parameters using PSO algorithm," *Renew. Energy*, vol. 78, pp. 105–113, Jun. 2015.

[10] M. C. D. Piazza, M. Luna, G. Petrone, and G. Spagnuolo, "Translation of the single-diode PV model parameters identified by using explicit formulas," *IEEE J. Photovolt.*, vol. 7, no. 4, pp. 1009–1016, Jul. 2017.

[11] A. Şentürk, "New method for computing single diode model parameters of photovoltaic modules," *Renew. Energy*, vol. 128, pp. 30–36, Dec. 2018.

[12] S. Lun, S. Wang, G. Yang, and T. Guo, "A new explicit double-diode modeling method based on Lambert W-function for photovoltaic arrays," *Sol. Energy*, vol. 116, pp. 69–82, Jun. 2015.

[13] F. J. Toledo, J. M. Blanes, and V. Galiano, "Two-step linear least-squares method for photovoltaic single-diode model parameters extraction," *IEEE Trans. Ind. Electron.*, vol. 65, no. 8, pp. 6301–6308, Aug. 2018.

[14] K. Et-torabi, I. Nassar-eddine, A. Obbadi, Y. Errami, R. Rmaily, S. Sahnoun, A. El Fajri, and M. Agunaou, "Parameters estimation of the single and double diode photovoltaic models using a Gauss–Seidel algorithm and analytical method: A comparative study," *Energy Convers. Manage.*, vol. 148, pp. 1041–1054, Sep. 2017.

[15] A. Yahya-Khotbehsara and A. Shahhoseini, "A fast modeling of the double-diode model for PV modules using combined analytical and numerical approach," *Sol. Energy*, vol. 162, pp. 403–409, Mar. 2018.

[16] A. Chatterjee, A. Keyhani, and D. Kapoor, "Identification of photovoltaic source models," *IEEE Trans. Energy Convers.*, vol. 26, no. 3, pp. 883–889, Sep. 2011.

[17] A. Ayang, R. Wamkeue, M. Ouhrouche, N. Djongyang, N. E. Salomé, J. K. Pombe, and G. Ekemb, "Maximum likelihood parameters estimation of single-diode model of photovoltaic generator," *Renew. Energy*, vol. 130, pp. 111–121, Jan. 2019.

[18] M. Zagrouba, A. Sellami, M. Bouaïcha, and M. Ksouri, "Identification of PV solar cells and modules parameters using the genetic algorithms: Application to maximum power extraction," *Sol. Energy*, vol. 84, no. 5, pp. 860–866, May 2010.

[19] L. Wu, Z. Chen, C. Long, S. Cheng, P. Lin, Y. Chen, and H. Chen, "Parameter extraction of photovoltaic models from measured I-V characteristics curves using a hybrid trust-region reflective algorithm," *Appl. Energy*, vol. 232, pp. 36–53, Dec. 2018.

[20] G. Xiong, J. Zhang, D. Shi, and Y. He, "Parameter extraction of solar photovoltaic models using an improved whale optimization algorithm," *Energy Convers. Manage.*, vol. 174, pp. 388–405, Oct. 2018.

[21] D. Oliva, M. Abd El Aziz, and A. Ella Hassanien, "Parameter estimation of photovoltaic cells using an improved chaotic whale optimization algorithm," *Appl. Energy*, vol. 200, pp. 141–154, Aug. 2017.

[22] A. M. Beigi and A. Maroosi, "Parameter identification for solar cells and module using a Hybrid firefly and pattern search algorithms," *Sol. Energy*, vol. 171, pp. 435–446, Sep. 2018.

[23] D. Kler, P. Sharma, A. Banerjee, K. P. S. Rana, and V. Kumar, "PV cell and module efficient parameters estimation using evaporation rate based water cycle algorithm," *Swarm Evol. Comput.*, vol. 35, pp. 93–110, Aug. 2017.

[24] R. Abbassi, A. Abbassi, A. A. Heidari, and S. Mirjalili, "An efficient salp swarm-inspired algorithm for parameters identification of photovoltaic cell models," *Energy Convers. Manage.*, vol. 179, pp. 362–372, Jan. 2019.

[25] K. Yu, B. Qu, C. Yue, S. Ge, X. Chen, and J. Liang, "A performance-guided JAYA algorithm for parameters identification of photovoltaic cell and module," *Appl. Energy*, vol. 237, pp. 241–257, Mar. 2019.

[26] D. F. Alam, D. A. Yousri, and M. B. Eteiba, "Flower pollination algorithm based solar PV parameter estimation," *Energy Convers. Manage.*, vol. 101, pp. 410–422, Sep. 2015.

[27] K. Yu, J. J. Liang, B. Y. Qu, Z. Cheng, and H. Wang, "Multiple learning backtracking search algorithm for estimating parameters of photovoltaic models," *Appl. Energy*, vol. 226, pp. 408–422, Sep. 2018.

[28] E. Ogliari, A. Niccolai, S. Leva, and E. R. Zich, "Computational intelligence techniques applied to the day ahead PV output power forecast: PHANN, SNO and Mixed," *Energies*, vol. 11, no. 1487, pp. 1–16, 2018.

[29] K. Yu, X. Chen, X. Wang, and Z. Wang, "Parameters identification of photovoltaic models using self-adaptive teaching-learning-based optimization," *Energy Convers. Manage.*, vol. 145, pp. 233–246, Aug. 2017.

[30] Q. Hao, Z. Zhou, Z. Wei, and G. Chen, "Parameters identification of photovoltaic models using a multi-strategy success-history-based adaptive differential evolution," *IEEE Access*, vol. 8, pp. 35979–35994, 2020.

[31] B. Subudhi and R. Pradhan, "Bacterial foraging optimization approach to parameter extraction of a photovoltaic module," *IEEE Trans. Sustain. Energy*, vol. 9, no. 1, pp. 381–389, Jan. 2018.

[32] V. J. Chin, Z. Salam, and K. Ishaque, "An accurate modelling of the two-diode model of PV module using a hybrid solution based on differential evolution," *Energy Convers. Manage.*, vol. 124, pp. 42–50, Sep. 2016.

[33] P. P. Biswas, P. N. Suganthan, G. Wu, and G. A. J. Amaratunga, "Parameter estimation of solar cells using datasheet information with the application of an adaptive differential evolution algorithm," *Renew. Energy*, vol. 132, pp. 425–438, Mar. 2019.

[34] H. M. Hasanien, "Shuffled frog leaping algorithm for photovoltaic model identification," *IEEE Trans. Sustain. Energy*, vol. 6, no. 2, pp. 509–515, Apr. 2015.

[35] G. F. Gomes, S. S. da Cunha, and A. C. Ancelotti, "A sunflower optimization (SFO) algorithm applied to damage identification on laminated composite plates," *Eng. Comput.*, vol. 35, no. 2, pp. 619–626, Apr. 2019.

[36] D. Allam, D. A. Yousri, and M. B. Eteiba, "Parameters extraction of the three diode model for the multi-crystalline solar cell/module using moth-flame optimization algorithm," *Energy Convers. Manage.*, vol. 123, pp. 535–548, Sep. 2016.
[37] H. M. Qais, M. H. Hasanien, S. Alghuwainem, and S. A. Nouh, "Coyote optimization algorithm for parameters extraction of three-diode photovoltaic model of photovoltaic modules," *Energy*, vol. 187, pp. 1–8, Nov. 2019.
[38] S. O. Elazab, M. H. Hasanien, I. Alsaidan, Y. A. Abdelaziz, and S. M. Muyeen, "Parameter estimation of three diode photovoltaic model using grasshopper optimization algorithm," *Energies*, vol. 13, no. 2, pp. 497–512, 2020.
[39] A. Faramarzi, M. Heidarinejad, S. Mirjalili, and A. H. Gandomi, "Marine predators algorithm: A nature-inspired metaheuristic," *Expert Syst. Appl.*, vol. 152, Aug. 2020, Art. no. 113377.
[40] D. Yousri, T. S. Babu, E. Beshr, M. B. Eteiba, and D. Allam, "A robust strategy based on marine predators algorithm for large scale photovoltaic array reconfiguration to mitigate the partial shading effect on the performance of PV system," *IEEE Access*, vol. 8, pp. 112407–112426, 2020.
[41] M. Abdel-Basset, R. Mohamed, M. Elhoseny, R. K. Chakrabortty, and M. Ryan, "A hybrid COVID-19 detection model using an improved marine predators algorithm and a ranking-based diversity reduction strategy," *IEEE Access*, vol. 8, pp. 79521–79540, 2020.
[42] A. A. M. Al-Qaness, A. A. Ewees, H. Fan, L. Abualigah, and M. A. Elaziz, "Marine predators algorithm for forecasting confirmed cases of COVID-19 in Italy, USA, Iran and Korea," *Int. J. Environ. Res. Public Health*, vol. 17, no. 10, pp. 1–14, 2020.
[43] W. De Soto, S. A. Klein, and W. A. Beckman, "Improvement and validation of a model for photovoltaic array performance," *Sol. Energy*, vol. 80, no. 1, pp. 78–88, Jan. 2006.
[44] D. Sera, R. Teodorescu, and P. Rodriguez, "PV panel model based on datasheet values," in *Proc. IEEE Int. Symp. Ind. Electron.*, Vigo, Spain, Jun. 2007, pp. 2392–2396.
[45] The Math Works Press. (Sep. 2016). *MATLAB*. Accessed: Sep. 13, 2017. [Online]. Available: https://www.mathworks.com/products/new_products/release2016b.html
[46] J. D. Filmalter, L. Dagorn, P. D. Cowley, and M. Taquet, "First descriptions of the behavior of silky sharks, carcharhinus falciformis, around drifting fish aggregating devices in the Indian Ocean," *Bull. Mar. Sci.*, vol. 87, no. 3, pp. 325–337, Jul. 2011.
[47] Kyocera. (2018). *KC200GT Kyocera PV Module Datasheet*. Accessed: Dec. 1, 2018. [Online]. Available: http://www.kyocera.com.sg/products/solar/pdf/kc200gt.pdf
[48] Solarex. (2018). *MSX-60 PV Module Solarex Datasheet*. Accessed: Dec. 1, 2018. [Online]. Available: http://www.solarelectricsupply.com/solarpanels/solarex/solarex-msx-60-w-junctionbox
[49] M. G. Villalva, J. R. Gazoli, and E. R. Filho, "Comprehensive approach to modeling and simulation of photovoltaic arrays," *IEEE Trans. Power Electron.*, vol. 24, no. 5, pp. 1198–1208, May 2009.

MAHMOUD A. SOLIMAN was born in Alexandria, Egypt, in December 1986. He received the B.Sc. (Hons.), M.Sc., and Ph.D. degrees in electrical engineering from the Faculty of Engineering, Menoufia University, Shebin El-Kom, Egypt, in 2008, 2013, and 2019, respectively. His Ph.D. research work is focused on the performance enhancement of the wind energy conversion systems. He joined Oil and Gas industry as an Electrical Engineer in 2009 up till now. Since 2013, he has been involved in scientific research of power electronics technology and renewable power generation systems. He is currently the Head of the Department of Dynamic Positioning and Navigation, Petroleum Marine Services Company, Alexandria. He is a Reviewer in different international journals, including the IET journals and the Elsevier journals. His research interests include electrical drives, modern control techniques, power factor correction converters, renewable energy systems, micro- and smart grids, flexible AC transmission system, HVDC systems, energy storage systems, and artificial intelligence applications on electrical machines and renewable energy systems.

HANY M. HASANIEN (Senior Member, IEEE) received the B.Sc., M.Sc., and Ph.D. degrees in electrical engineering from the Faculty of Engineering, Ain Shams University, Cairo, Egypt, in 1999, 2004, and 2007, respectively. From 2008 to 2011, he was a Joint Researcher with the Kitami Institute of Technology, Kitami, Japan. From 2012 to 2015, he was an Associate Professor with the College of Engineering, King Saud University, Riyadh, Saudi Arabia. He is currently a Professor with the Department of Electrical Power and Machines, Faculty of Engineering, Ain Shams University. He has published more than 150 articles in international journals and conferences. He has authored, coauthored, and edited three books in the field of electric machines and renewable energy. His research interests include modern control techniques, power systems dynamics and control, energy storage systems, renewable energy systems, and smart grid. His biography has been included in Marquis Who's Who in the world for its 28 edition, in 2011. He was awarded Encouraging Egypt Award for Engineering Sciences in 2012. He was awarded Institutions Egypt Award for Invention and Innovation of Renewable Energy Systems Development in 2014. He is also the IEEE PES Egypt Chapter Chair. He is an Editorial Board Member of *Electric Power Components and Systems Journal*. He is a Subject Editor of *IET Renewable Power Generation*, *Ain Shams Engineering Journal*, and *Electronics* MDPI.

ABDULAZIZ ALKUHAYLI (Member, IEEE) received the B.Sc. degree in electrical engineering from King Saud University, Riyadh, Saudi Arabia, in 2006, the M.S. degree in electrical engineering from the Missouri University of Science and Technology, Rolla, MO, USA, in 2013, and the Ph.D. degree in electrical engineering from North Carolina State University, Raleigh, NC, USA, in 2018. From 2006 to 2009, he worked as an Operation Engineer with the Energy Control Center, Saudi Electricity Company. He is currently an Assistant Professor with the Department of Electrical Engineering, King Saud University. His research interests include energy management, renewable energy systems, flexible AC transmission systems, power system stability, and smart grid.